2018

Biomimetic aquaporin membranes for osmotic membrane bioreactors: Membrane performance and contaminant removal

Wenhai Luo
University of Wollongong, China Agricultural University, wl344@uowmail.edu.au

Ming Xie
Victoria University, mx504@uowmail.edu.au

Xiaoye Song
University of Wollongong, xs245@uowmail.edu.au

Wenshan Guo
University of Technology Sydney, wguo@uts.edu.au

Hao H. Ngo
University of Technology Sydney, h.ngo@uts.edu.au

See next page for additional authors

Biomimetic aquaporin membranes for osmotic membrane bioreactors: Membrane performance and contaminant removal

Abstract

In this study, we investigated the performance of an osmotic membrane bioreactor (OMBR) enabled by a novel biomimetic aquaporin forward osmosis (FO) membrane. Membrane performance and removal of 30 trace organic contaminants (TrOCs) were examined. Results show that the aquaporin FO membrane had better transport properties in comparison with conventional cellulose triacetate and polyamide thin-film composite FO membranes. In particular, the aquaporin FO membrane exhibited much lower salt permeability and thus smaller reverse salt flux, resulting in a less severe salinity build-up in the bioreactor during OMBR operation. During OMBR operation, the aquaporin FO membrane well complemented biological treatment for stable and excellent contaminant removal. All 30 TrOCs selected here were removed by over 85% regardless of their diverse properties. Such high and stable contaminant removal over OMBR operation also indicates the stability and compatibility of the aquaporin FO membrane in combination with activated sludge treatment.

Disciplines

Engineering | Science and Technology Studies

Publication Details

Luo, W., Xie, M., Song, X., Guo, W., Ngo, H. H., Zhou, J. L. & Nghiem, L. D. (2018). Biomimetic aquaporin membranes for osmotic membrane bioreactors: Membrane performance and contaminant removal. Bioresource Technology, 249 62-68.

Authors

Wenhai Luo, Ming Xie, Xiaoye Song, Wenshan Guo, Hao H. Ngo, John L. Zhou, and Long D. Nghiem

Biomimetic aquaporin membranes for osmotic membrane bioreactors: Membrane performance and contaminant removal

Bioresource Technology 249 (2018) 62 – 68

Wenhai Luo [a,c*], Ming Xie [b], Xiaoye Song [c], Wenshan Guo [d], Hao H. Ngo [d], Junliang Zhou [d], Long D. Nghiem [c]

[a] *Beijing Key Laboratory of Farmland Soil Pollution Prevention and Remediation, College of Resources and Environmental Sciences, China Agricultural University, Beijing, 100193, China*

[b] *Institute for Sustainability and Innovation, College of Engineering and Science, Victoria University, Melbourne, VIC 8001, Australia*

[c] *Strategic Water Infrastructure Laboratory, School of Civil, Mining and Environmental Engineering, University of Wollongong, Wollongong, NSW 2522, Australia*

[d] *Centre for Technology in Water and Wastewater, School of Civil and Environmental Engineering, University of Technology Sydney, Sydney, NSW 2007, Australia*

[*] Corresponding author: luowenhai@cau.edu.cn; Ph: +86 18311430503.

Abstract

In this study, we investigated the performance of an osmotic membrane bioreactor (OMBR) enabled by a novel biomimetic aquaporin forward osmosis (FO) membrane. Membrane performance and removal of 30 trace organic contaminants (TrOCs) were examined. Results show that the aquaporin FO membrane had better transport properties in comparison with conventional cellulose triacetate and polyamide thin-film composite FO membranes. In particular, the aquaporin FO membrane exhibited much lower salt permeability and thus smaller reverse salt flux, resulting in a less severe salinity build-up in the bioreactor during OMBR operation. During OMBR operation, the aquaporin FO membrane well complemented biological treatment for stable and excellent contaminant removal. All 30 TrOCs selected here were removed by over 85% regardless of their diverse properties. Such high and stable contaminant removal over OMBR operation also indicates the stability and compatibility of the aquaporin FO membrane in combination with activated sludge treatment.

Keywords: Aquaporin membrane; forward osmosis; osmotic membrane bioreactor; trace organic contaminant; activated sludge treatment

1. Introduction

Membrane bioreactors (MBRs), which integrate physical membrane separation process, such as microfiltration (MF) and ultrafiltration (UF), with conventional activated sludge (CAS) treatment, have been widely deployed for wastewater treatment and reuse. Compared to CAS treatment, MBRs have several advantages, including better effluent quality, lower sludge production, smaller footprint, and easier operation and maintenance (Huang & Lee, 2015). For wastewater reuse that requires high water quality, further treatment, for example, by nanofiltration, reverse osmosis (RO), and advanced oxidation, is still necessary (Elimelech, 2006; Shannon et al., 2008; van Loosdrecht & Brdjanovic, 2014).

Forward osmosis (FO), an osmosis-driven process, was proposed recently to integrate with CAS to form a novel MBR, namely, osmotic MBR or OMBR (Achilli et al., 2009; Cornelissen et al., 2011; Holloway et al., 2015; Aftab et al., 2017). During OMBR operation, treated water from the bioreactor permeates through a semi-permeable FO membrane into a draw solution using osmotic pressure difference across the membrane as the driving force. A draw solution regeneration process, such as RO or membrane distillation (MD), can then be used to re-concentrate the draw solution and produce clean water for reuse applications (Holloway et al., 2014; Nguyen et al., 2016). By utilizing the osmotic pressure-driven process, OMBR can be a low fouling alternative to conventional MBR, in which hydraulically driven MF or UF membranes are commonly equipped (Achilli et al., 2009). Moreover, it has been demonstrated that membrane fouling of the RO process after OMBR is significantly less than that after conventional MBR (Luo et al., 2017). Unlike MF and UF membranes used in conventional MBR, FO membranes have a high rejection capacity for most contaminants, including trace organic contaminants (TrOCs) that remain vexing challenges to water reuse applications (Alturki et al., 2012; Holloway et al., 2014). Thus, OMBR can produce higher quality effluent in comparison to conventional MBR (Luo et al., 2017).

One critical issue in OMBR operation is salinity build-up in the bioreactor, which could alter sludge characteristics, inhibit biological activity, and thus deteriorate OMBR performance (Luo et al., 2017). Such unfavorable salinity build-up was driven by the high salt rejection by the FO membrane, and more importantly, the reverse draw solute permeation into the bioreactor. Despite the advancement in FO membranes from cellulose triacetate (CTA) to polyamide thin-film composite (TFC) (Fane et al., 2015; Werber et al., 2016), salinity build-up remains hindrance to the further development and deployment of OMBR. Thus, recent efforts have been dedicated to control salinity build-up during OMBR operation by periodically discharging mixed liquor (Wang et al., 2014a), integrating with porous membranes for salt bleeding (Wang et al., 2014b; Holloway et al., 2015), and employing biodegradable draw solutes (Bowden et al., 2012; Luo et al., 2016a). However, these strategies cannot completely address the issue of salinity build-up in OMBR. Indeed, the development of novel FO membranes with low salt permeability is the most effective to control salinity build-up (Fane et al., 2015).

Biomimetic membranes, based on aquaporins, have the potential to further advance FO and OMBR processes (Tang et al., 2015; Li et al., 2016; Giwa et al., 2017). Aquaporins are water-channel proteins in biological cell membrane. Each aquaporin channel is capable of transporting up to 10^9 water molecules per second and absolute rejection of all other solutes (Jensen & Mouritsen, 2006). Madsen et al. (2015) reported that the aquaporin FO membrane exhibited nearly 97% rejection of three neutral TrOCs, namely atrazine, 2,6-dichlorobenzamide and desethyl-desisopropyl-atrazine. By introducing aquaporins into polymeric membranes, the permeability-selectivity trade-off of conventional TFC membranes could be considerably overcome (Li et al., 2015). Li et al. (2017) reported that incorporating aquaporin proteins into the polyamide selective layer of a hollow fiber TFC FO membrane could largely increase the membrane water flux while reduce the reverse salt flux. Nevertheless, there is a dearth in current literature on the performance of

biomimetic FO membranes in OMBR operation, where the biocompatibility of these newly developed membranes is challenged.

In this study, the performance of an aquaporin-based biomimetic FO membrane in OMBR operation was investigated. Key properties of the aquaporin membrane were characterized and compared to conventional CTA and TFC FO membranes. The aquaporin membrane performance in OMBR operation was evaluated in terms of water flux, bioreactor salinity, and contaminant removal. Role of the aquaporin FO membrane in OMBR for TrOC removal was also quantified. Results from this study provide important implications to examine the compatibility and potential of biomimetic aquaporin membranes for OMBR applications.

2. Materials and methods

2.1 Synthetic wastewater and trace organic contaminants

A synthetic wastewater was used as the OMBR influent. This synthetic wastewater was prepared daily and consisted of 100 mg/L glucose, 100 mg/L peptone, 17.5 mg/L KH_2PO_4, 17.5 mg/L $MgSO_4$, 17.5 mg/L $CaCl_2$, 10 mg/L $FeSO_4$, 225 mg/L CH_3COONa, and 35 mg/L urea. Key physicochemical properties of the synthetic wastewater were determined every three days. In particular, the synthetic wastewater contained 111.3 ± 13 mg/L total organic carbon (TOC), 6.4 ± 0.9 mg/L total nitrogen (TN), 4.1 ± 0.45 mg/L ammonium nitrogen (NH_4^+), and 10.9 ± 2.5 mg/L phosphate (PO_4^{3-}). The electrical conductivity and pH of this synthetic wastewater were 321 ± 15 µS/cm and 6.2 ± 0.3, respectively.

A set of 30 TrOCs were selected to represent emerging chemicals of significant concern that ubiquitously present in municipal wastewater. A stock solution containing 25 µg/mL of each of TrOCs was prepared in pure methanol and stored at -18 °C in the dark. The stock solution was introduced daily to the synthetic wastewater to obtain a concentration of 5 µg/L of each compound.

2.2 Biomimetic aquaporin FO membrane

119 A flat-sheet aquaporin FO membrane obtained from Aquaporin Asia, Singapore was
120 used in this study. The biomimetic FO membrane was fabricated via interfacial
121 polymerization with embedded aquaporin proteins vesicles into a polyamide selective
122 layer supported by a porous polysulfone supporting layer (Madsen et al., 2015).

123 Conventional CTA and TFC FO membranes obtained from Hydration Technology
124 Innovation (Albany, OR) were also used in this study as benchmarks. The CTA
125 membrane was fabricated via phase inversion and composed of a cellulose triacetate
126 layer with an embedded woven supporting mesh. The TFC membrane was made by
127 interfacial polymerization with a thin, selective polyamide active layer on the top of a
128 porous polysulfone supporting layer (Cath et al., 2013).

129 *2.3 Osmotic membrane bioreactor*

130 A lab-scale, submerged OMBR system was used (Fig. 1). This system mainly
131 comprised a glass bioreactor, a plate-and-frame FO membrane module, and a draw
132 solution delivery and control unit. A peristaltic pump (Cole-Parmer, Vernon Hills, IL)
133 controlled by a water level sensor was used to feed synthetic wastewater into the
134 bioreactor. The membrane module was made of acrylic plastic and had a draw
135 solution flow chamber with a length, width, and height of 150, 80, and 3 mm,
136 respectively. The FO membrane was sealed on the draw solution flow chamber with
137 the active layer facing the mixed liquor and an effective area of 120 cm^2. A gear pump
138 (Micropump, Vancouver, WA) was used to circulate the draw solution to the
139 membrane cell at a cross-flow rate of 0.75 L/min, corresponding to a cross-flow
140 velocity of 5.2 cm/s.

141 **[Figure 1]**

142 The draw solution reservoir was placed on a digital balance (Mettler-Toledo,
143 Hightstown, USA) connected to a computer. An increase in the draw solution weight
144 was recorded and used to determine the OMBR water flux. The draw solution
145 concentration was maintained using a conductivity controller unit and a highly

146 concentrated draw solution. A detailed description of the conductivity controller has
147 been reported in our previous study (Luo et al., 2015). Briefly, the conductivity
148 controller was consisted of a conductivity probe, a conductivity sensor, and a small
149 peristaltic pump. The concentrated draw solution reservoir was also placed on the
150 same digital balance with the working draw solution tank to avoid interference in
151 water flux calculation.

152 *2.4 Operation of osmotic membrane bioreactor*

153 Activated sludge obtained from a conventional, lab-scale MBR was used to inoculate
154 the OMBR system. The conventional MBR had been acclimatized to laboratory
155 conditions and the synthetic wastewater for more than three months. Stable
156 performance of the conventional MBR had achieved as indicated by its relatively
157 constant and effective removal of total organic carbon (TOC) (>95%). The initial
158 mixed liquor suspended solid concentration (MLSS) of OMBR was adjusted to
159 approximately 7 g/L. The bioreactor had an effective volume of 4 L and was
160 continuously aerated to obtain a dissolved oxygen (DO) concentration of above 2
161 mg/L. The operating sludge retention time (SRT) was maintained at 20 days by daily
162 withdrawing 200 mL mixed liquor. A 0.5 M NaCl solution was used as the draw
163 solution whose concentration was maintained by the conductivity controller
164 equipment and a 6 M NaCl solution. The working draw solution was replaced on a
165 daily basis to avoid contaminant accumulation and overflow. The operating hydraulic
166 retention time (HRT) was determined by the FO water flux and was in the range of 24
167 – 36 hours, resulting in the system organic loading rate in the range of 74 – 109 g
168 TOC/(m^3d). The OMBR system was continuously operated for 20 days in a
169 temperature-controlled room (22 ± 1 °C). No membrane clean was conducted
170 throughout the experiment.

171 *2.5 Analytical methods*

172 *2.5.1 Membrane transport parameters*

Membrane transport parameters were determined based on the standard methodology reported by Cath et al. (2013). Briefly, the water permeability coefficient (A) and salt (NaCl) permeability coefficient (B) was examined using a cross-flow RO system with deionized water and 2,000 mg/L NaCl solution as the feed solution, respectively. The RO water flux was recorded at an applied hydraulic pressure (ΔP) of 10 bar and a cross-flow velocity of 25 cm/s. Both feed and permeate samples were taken to determine the observed NaCl rejection (R_{ob}). The A and B values were calculated as follows:

$$A = \frac{J_{RO}}{\Delta P} \tag{1}$$

$$B = J_{NaCl}\left(\frac{1 - R_{ob}}{R_{ob}}\right) exp\left(-\frac{J_{NaCl}}{k_f}\right) \tag{2}$$

where J_{RO} and J_{NaCl} was the RO water flux (L/m^{2}h) with deionized water and NaCl solution as the feed solution, respectively; k_f was the mass transfer coefficient of the cross-flow RO membrane cell (μm/s), which was determined using the salt concentration at the membrane surface with the film theory for concentration polarization (Sutzkover et al., 2000):

$$k_f = \frac{J_{NaCl}}{ln\left[\frac{\Delta P}{\pi_b - \pi_p}\left(1 - \frac{J_{NaCl}}{J_{RO}}\right)\right]} \tag{3}$$

where π_p and π_b was the feed and permeate osmotic pressure (bar), respectively. They were determined by their salt concentrations according to the van't Hoff equation.

Membrane structural parameter (S), which indicates the content of internal concentration polarization of the FO membrane, is defined as follows:

$$S = \frac{l\tau}{\varepsilon} \tag{4}$$

where l is the supporting layer thickness, τ is the supporting layer tortuosity, and ε is the supporting layer porosity.

196 Membrane S value was experimentally determined using a cross-flow FO system with
197 0.5 M NaCl draw solution and deionized water feed in this study. Water flux (J_{FO}) was
198 recorded after stabilizing the system for two hours for S value calculation based on the
199 following equation:

200 $$S = \frac{D_s}{J_{FO}} ln\left(\frac{B + A\pi_{D,b}}{B + J_{FO} + A\pi_{F,m}}\right) \quad (5)$$

201 where D_s was the draw solute diffusivity (m^2/s); $\pi_{D,b}$ was the draw solution osmotic
202 pressure (bar); and $\pi_{F,m}$ was the osmotic pressure at the membrane surface on the feed
203 side (zero for deionized water feed).

204 *2.5.2 Membrane surface charge, morphology, and hydrophobicity*

205 Membrane surface charge was measured by a SurPASS electrokinetic analyzer (Anton
206 Paar CmbH, Graz, Austria). Zeta potential of the membrane surface was calculated
207 from the measured streaming potential using the Fairbrother-Maastin approach
208 (Elimelech et al., 1994). All streaming potential measurements were performed in a
209 background electrolyte solution (i.e. 10 mM KCl). The background solution was also
210 used to completely flush the cell before pH titration using either 0.5 M hydrochloric
211 acid or 0.5 M potassium hydroxide.

212 A scanning electron microscopy (SEM) coupled with energy dispersive spectroscopy
213 (EDS) (JCM-6000, JEOL, Tokyo, Japan) was used to characterize the membrane
214 surface morphology and elementary composition. Prior to the SEM measurement,
215 air-dried membrane samples were coated with an ultra-thin layer of gold using a
216 sputter coater (SPI Module, West Chester, PA).

217 Membrane hydrophobicity was assessed by contact angle measurements using a
218 Rame-Hart Goniometer (Model 250, Rame-Hart, Netcong, NJ) based on the standard
219 sessile drop method. Ten water droplets were applied to each dried membrane sample.
220 Contact angles on both sides of the droplet were recorded.

221 *2.5.3 Basic water quality parameters*

222 Total organic carbon (TOC) and total nitrogen (TN) were analyzed using a TOC/TN
223 analyzer (TOC-V_{CSH}, Shimadzu, Kyoto). Ammonium (NH_4^+) and orthophosphate
224 (PO_4^{3-}) were measured by a flow injection analysis system (QuikChem 8500, Lachat,
225 CO). Removal of these contaminants by OMBR was determined based on the method
226 described in the following section. An Orion 4-Star Plus pH/conductivity meter
227 (Thermo Scientific, Waltham, MA) was used to measure the solution pH and
228 electrical conductivity.

229 *2.5.4 Analysis of trace organic contaminants*

230 TrOC concentrations in wastewater, mixed liquor supernatant, and draw solution were
231 analyzed every five days based on an analytic method reported by Hai et al. (2011).
232 Briefly, this method involved solid phase extraction, derivatization, and quantification
233 by a gas chromatography – mass spectrometry system (QP5000 GC-MS, Shimadzu,
234 Kyoto).

235 Contaminant removal by OMBR was determined based on the method reported in our
236 previous study (Luo et al., 2015). Briefly, a dilution factor (*DF*) was used to correct
237 the draw solution dilution in calculating TrOC concentrations in the FO permeate:

238 $$DF = \frac{V_{Draw}}{V_{FO}} \quad (6)$$

239 where V_{Draw} and V_{FO} was the volume of the draw solution and water permeated
240 through the FO membrane, respectively, when TrOC samples were collected for
241 analysis.

242 TrOC removal by OMBR could be defined as follows:

243 $$R_{OMBR} = (1 - \frac{C_{Draw}}{C_{Feed}} DF) \times 100\% \quad (7)$$

244 where C_{Feed} and C_{Draw} was the measured TrOC concentration in the feed and draw
245 solution, respectively.

246 TrOC removal by OMBR was the complementary result of biological degradation and
247 aquaporin FO membrane rejection. Thus, biological removal of TrOCs (R_{Bio}) was
248 defined as:

249 $$R_{Bio} = (1 - \frac{C_{Sup}V_{Bio} + C_{Draw}DF\ \Delta V_{FO}}{C_{Feed}\Delta V}) \times 100\% \quad (8)$$

250 where C_{Sup} was the TrOC concentration measured in the mixed liquor supernatant;
251 V_{Bio} was the effective bioreactor volume; and ΔV_{FO} was the volume of water
252 permeated through the FO membrane between time t and t-Δt, which was equal to the
253 volume of wastewater fed into the bioreactor (ΔV).

254 Based on eqs. (7) and (8), the observed rejection of TrOCs by the aquaporin FO
255 membrane ($R_{Ob\ FO}$) was defined as follows:

256 $$R_{Ob\ FO} = R_{OMBR} - R_{Bio} \quad (4)$$

257 It is noteworthy that the observed rejection rate could not show the real rejection
258 capacity of the aquaporin FO membrane, but quantify its contribution toward TrOC
259 removal in OMBR.

260 **3. Results and discussion**

261 *3.1 Key properties of the aquaporin FO membrane*

262 Key properties of the aquaporin FO membrane were evaluated and compared to CTA
263 and TFC FO membranes currently available in the market. Water permeability
264 coefficient (A value) of the aquaporin membrane was significantly higher than that of
265 the CTA membrane, but was comparable or only slightly lower than that of the TFC
266 membrane (Table 1). This observation could be attributed to the difference in their
267 membrane structural parameter (S value) (Table 1), which indicates the extent of the
268 internal concentration polarization in the FO process (McCutcheon & Elimelech,
269 2006). As a result, the aquaporin and TFC membranes exhibited high and comparable
270 water flux of approximately 15.6 and 15 L/m^{2}h, respectively, in the cross-flow FO

experiment with 0.5 NaCl draw solution and deionized water feed solution. On the other hand, the CTA membrane showed a much lower water flux of 5.5 L/m^{2}h under the same testing condition.

[Table 1]

By incorporating highly selective aquaporin vesicles into membrane active layer, the aquaporin FO membrane showed much lower salt (NaCl) permeability (*B* value) than both CTA and TFC membranes (Table 1). Thus, the reverse salt (NaCl) flux of the aquaporin membrane was 0.085 mmol/hm^2, which was considerably lower than that of the CTA (82.7 mmol/hm^2) and TFC (5.5 mmol/hm^2) membranes, in the cross-flow FO experiment with 0.5 NaCl draw and deionized water feed. Moreover, the aquaporin FO membrane also demonstrated an excellent capacity for salt (NaCl) rejection (Table 1). Compared to the CTA and TFC membranes, the aquaporin FO membrane was more negatively charged and hydrophobic (Table 1), possibly due to the physical features of lipid vesicles immobilized into the membrane selective layer (Xie et al., 2013).

3.2 Performance of the aquaporin FO membrane in OMBR operation

3.2.1 Salinity build-up and water production

Salinity build-up in the bioreactor is an inherent issue associated with OMBR operation, due to the high salt rejection from wastewater by the FO membrane, and more importantly, the reverse draw solute diffusion (Lay et al., 2010). As discussed above, the reverse salt flux through the aquaporin FO membrane was insignificant (Table 1). Thus, the observed salinity increase in the bioreactor from approximately 0.4 to 8.6 mS/cm within 20 days of OMBR operation (Fig. 2) can be attributed mostly to the build-up of salts originally from the influent. Indeed, this salinity increase was less severe when comparing to previous OMBR studies using conventional CTA and TFC FO membranes under similar operating conditions. For example, Luo et al. (2017) observed an increase in the mixed liquor conductivity from 0.3 to nearly 11

298 mS/cm within 20 days during OMBR operation with the conventional TFC FO
299 membrane.

300 **[Figure 2]**

301 Water flux of the aquaporin FO membrane decreased continuously during OMBR
302 operation (Fig. 2). This observation is consistent with that reported previously and
303 could be attributed to salinity build-up in the bioreactor and membrane fouling (Xiao
304 et al., 2011; Wang et al., 2016). Salinity build-up in the bioreactor could increase the
305 osmotic pressure in the mixed liquor side and thus reduce the net driving force (i.e.
306 effective trans-membrane osmotic pressure) for water permeation (Xiao et al., 2011).

307 With osmotic pressure as the driving force, FO has relatively low fouling propensity
308 and high fouling reversibility in wastewater treatment (Mi & Elimelech, 2010).
309 Moreover, in this study, routine approach was used in OMBR operation where
310 continuous aeration required for sludge growth and metabolism could produce air
311 bubbles to alleviate the formation and attachment of cake layer on the membrane
312 surface. However, a patchy and thin fouling layer, mainly consisted of carbon,
313 nitrogen, oxygen, and sulfur, was observed on the aquaporin membrane surface at the
314 conclusion of OMBR operation. More significant fouling was formed in the upper
315 region of the membrane, where air bubbling was weakened by passing through the
316 mixed liquor (Braak et al., 2011).

317 *3.2.2 Removal of bulk organic matter and nutrients*

318 By coupling biological treatment with highly selective aquaporin FO membrane,
319 OMBR could effectively remove organic matter and nutrients (Fig. 3). Despite
320 salinity build-up in the bioreactor (Fig. 2), biological treatment was stable during
321 OMBR operation, as indicated by negligible TOC and NH_4^+ concentrations in the
322 mixed liquor (Fig. 3A&B). Moreover, the MLSS concentration and the specific
323 oxygen uptake rate of activated sludge were relatively constant in OMBR operation,
324 corroborating stable biomass growth and activity. Indeed, most microorganisms in

325 activated sludge are non-halophilic and able to tolerate salinity up to 10 g/L NaCl
326 without acclimatization (Woolard & Irvine, 1995; Lay et al., 2010). Nevertheless,
327 salinity build-up in the bioreactor needs to be controlled to circumvent adverse effects
328 on biological treatment for sustainable OMBR operation, since higher saline
329 conditions (>10 g/L NaCl) can result in cell dehydration, and eventually, the
330 plasmolysis and inactivity of microorganisms in activated sludge (Lay et al., 2010).

331 **[Figure 3]**

332 Without denitrification under aerobic condition, TN removal by activated sludge is
333 commonly ineffective and only dependent on microbial assimilation (Gerrity et al.,
334 2013). Thus, in this study, only 60 – 80% TN was removed by OMBR (Fig. 3C),
335 which could be attributed mainly to the rejection of nitrogen species by the aquaporin
336 FO membrane. Indeed, although there were several fluctuations, TN concentration
337 increased in the mixed liquor. Nevertheless, a decrease in TN removal was observed
338 at the end of OMBR operation, indicating that the aquaporin FO membrane had a
339 moderate capacity for the rejection of nitrogen species, especially nitrate that could be
340 converted from NH_4^+ by complete nitrification under aerobic condition. Similar
341 results were also reported in previous OMBR studies with conventional CTA and TFC
342 FO membranes (Zhang et al., 2017).

343 Phosphorus removal in biological treatment also depends on microbial assimilation,
344 especially by phosphate accumulating microorganisms (PAOs) (Seviour et al., 2003).
345 However, the activity and metabolism of PAOs could be easily inhibited in saline
346 environment (Panswad & Anan, 1999). It has been reported that increased salinity in
347 sequencing batch reactor (Uygur & Karg, 2004) and conventional MBR (Luo et al.,
348 2016b) led to a dramatic and continuous decrease in phosphorus removal.
349 Nevertheless, given their relatively large hydrated radius and negative charge, PO_4^{3-}
350 ions were effectively rejected by the aquaporin FO membrane and thus accumulated
351 considerably in the mixed liquor, with negligible permeation into the draw solution
352 (Fig. 3D).

353 *3.2.3 Removal of trace organic contaminants*

354 All 30 TrOCs investigated in this study could be effectively removed (>85%) by
355 OMBR (Fig. 4), due to the complementarity of biological treatment and highly
356 selective aquaporin FO membrane. As shown in Fig. 4, biological treatment played
357 the dominating role for the removal of most TrOCs, with a few exceptions, such as
358 clofibric acid, carbamazepine, and atrazine. This removal deviation could be
359 attributed to the different properties of these TrOCs, such as hydrophobicity and
360 molecular feature. Based on a predictive protocol reported by Tadkaew et al. (2011),
361 the effective octanol – water partition coefficient (i.e. Log *D*) at the mixed liquor pH
362 of 8 was used to classify the 30 TrOCs as hydrophilic (Log $D < 3.2$) and hydrophobic
363 (Log $D > 3.2$).

364 **[Figure 4]**

365 All hydrophobic TrOCs (Log $D > 3.2$) could be effectively removed by activated
366 sludge, with removal rates higher than 90% (Fig. 4). Due to their hydrophobic
367 interactions with sludge, for example, via their aliphatic and aromatic functional
368 groups with the lipid fraction of sludge, hydrophobic TrOCs could easily absorb onto
369 activated sludge for further biodegradation (Besha et al., 2017). As a result, the
370 contribution of the aquaporin FO membrane to the overall removal of hydrophobic
371 TrOCs in OMBR was insignificant (less than 5%).

372 Removal of hydrophilic TrOCs (Log $D < 3.2$) via biological treatment varied
373 considerably (Fig. 4), depending on their intrinsic biodegradability. Some compounds
374 were removed by more than 80% in the bioreactor. These TrOCs include salicylic acid,
375 ketoprofen, naproxen, metronidazole, ibuprofen, gemfibrozil, pentachlorophenol,
376 DEET, and ametryn. On the other hand, poor removals were observed for several
377 other TrOCs, including clofibric acid, fenoprop, primidone, carbamazepine, and
378 atrazine, with removal rates less than 30%. This removal difference was in good
379 agreement with that reported previously in conventional MBR studies (Kimura et al.,

380 2005; Besha et al., 2017), and could be further attributed to different functional
381 groups in the molecular structure of these hydrophilic compounds. In general,
382 hydrophilic TrOCs containing strong electron-donating functional groups (e.g. amine
383 and hydroxyl) could be effectively biodegraded, due to their preferential to initial
384 electrophilic attack by oxygenase of aerobic bacteria; while compounds with
385 electron-withdrawing functional groups (e.g. chloro, amide, and nitro) were
386 recalcitrant to biodegradation, because these functional groups could generate electron
387 deficiency and thus constrain the oxidative catabolism of compounds (Knackmuss,
388 1996; Tadkaew et al., 2011).

389 The aquaporin FO membrane complemented well biological treatment to ensure
390 effective TrOC removal by OMBR, with significant contribution toward the removal
391 of hydrophilic and biologically persistent compounds (Fig. 4). This result was
392 consistent with that reported in previous OMBR studies, where the role of
393 conventional CTA and TFC FO membranes for TrOC removal was investigated (Luo
394 et al., 2017; Zhang et al., 2017). Although there is no direct comparison, the aquaporin
395 FO membrane should be able to make more contribution than these two conventional
396 FO membranes to increase the removal of hydrophilic and biologically recalcitrant
397 TrOCs in OMBR given its higher solute rejection capacity (Table 1). Indeed, Zhang et
398 al. (2017) demonstrated that the highly selective TFC FO membrane could enhance
399 the removal hydrophilic and biologically persistent TrOCs by OMBR in comparison
400 with the CTA FO membrane. It is noteworthy that the stable and high removal of
401 TrOCs observed in this study also suggested the robustness and stability of the
402 aquaporin FO membrane when integrated with activated sludge treatment.

403 **4. Implications**

404 Proteoliposomes (i.e. lipid vesicles with aquaporin proteins) are typically incorporated
405 into the dense polymeric matrix to strengthen biomimetic aquaporin membranes
406 (Zhao et al., 2012; Giwa et al., 2017). The aquaporin FO membrane used in this study
407 was fabricated via interfacial polymerization with proteoliposomes embedded into a

408 polyamide selective layer supported by a porous polysulfone supporting layer
409 (Madsen et al., 2015). Indeed, the SEM micrograph of the aquaporin FO membrane
410 showed that round-shape nodules, possibly aquaporin proteins vesicles, were covered
411 by the leaf-like polyamide structure. Further analysis of the membrane cross-section
412 by the transmission electron microscopy also demonstrated the embedment of
413 round-shape nodules within the membrane interface. Thus, the polyamide selective
414 layer could prevent proteoliposomes from biological degradation, endowing the
415 aquaporin FO membrane with an uncompromised performance in OMBR operation
416 (indicated by the stable and high contaminant removal). A stable performance of
417 biomimetic aquaporin membranes was also demonstrated in long-term RO
418 desalination (over 100 days) with periodical membrane cleaning by chemical agents
419 (Qi et al., 2016). Although long-term studies are necessary to valid the stability of
420 biomimetic aquaporin membranes against biological damage, this study shed light on
421 their promising potential in OMBR applications.

422 **5. Conclusion**

423 Results reported here demonstrate the potential of biomimetic aquaporin membranes
424 for OMBR application. Compared to conventional CTA and TFC FO membranes, the
425 aquaporin FO membrane exhibited much better transport properties, particularly
426 smaller reverse salt flux without compromising water permeation, which thereby
427 resulted in less severe salinity build-up in the bioreactor during OMBR operation.
428 Moreover, the aquaporin FO membrane could complement well biological treatment
429 for excellent contaminant removal in OMBR, with notable contribution towards the
430 removal of biologically persistent TrOCs. Stable contaminant removal over OMBR
431 operation also suggests the compatibility of the aquaporin FO membrane with
432 activated sludge treatment.

433 **6. Acknowledgements**

This research was supported under the Australian Research Council's Discovery Project funding scheme (Project DP140103864) and National Natural Science Foundation of China (Project 51708547). Dr. Jinguo Kang is gratefully acknowledged for his assistance with the analysis of trace organic contaminants.

7. Acknowledgements

Supplementary data of this study can be found in the e-version of this paper online.

8. References

1. Achilli, A., Cath, T.Y., Marchand, E.A., Childress, A.E. 2009. The forward osmosis membrane bioreactor: A low fouling alternative to MBR processes. Desalination, 239(1), 10-21.
2. Aftab, B., Khan, S.J., Maqbool, T., Hankins, N.P. 2017. Heavy metals removal by osmotic membrane bioreactor (OMBR) and their effect on sludge properties. Desalination, 403, 117-127.
3. Alturki, A.A., McDonald, J., Khan, S.J., Hai, F.I., Price, W.E., Nghiem, L.D. 2012. Performance of a novel osmotic membrane bioreactor (OMBR) system: Flux stability and removal of trace organics. Bioresour. Technol., 113, 201-206.
4. Besha, A.T., Gebreyohannes, A.Y., Tufa, R.A., Bekele, D.N., Curcio, E., Giorno, L. 2017. Removal of emerging micropollutants by activated sludge process and membrane bioreactors and the effects of micropollutants on membrane fouling: A review. J. Environ. Chem. Eng., 5(3), 2395-2414.
5. Bowden, K.S., Achilli, A., Childress, A.E. 2012. Organic ionic salt draw solutions for osmotic membrane bioreactors. Bioresour. Technol., 122, 207-216.
6. Braak, E., Alliet, M., Schetrite, S., Albasi, C. 2011. Aeration and hydrodynamics in submerged membrane bioreactors. J. Membr. Sci., 379(1-2), 1-18.
7. Cath, T.Y., Hancock, N.T., Lampi, J., Nghiem, L.D., Xie, M., Yip, N.Y., Elimelech, M., McCutcheon, J.R., McGinnis, R.L., Achilli, A., Anastasio, D., Brady, A.R., Childress, A.E., Farr, I.V. 2013. Standard methodology for

461 evaluating membrane performance in osmotically driven membrane processes.
462 Desalination, 312, 31-38.
463 8. Cornelissen, E.R., Harmsen, D., Beerendonk, E.F., Qin, J.J., Oo, H., De Korte,
464 K.F., Kappelhof, J.W.M.N. 2011. The innovative osmotic membrane bioreactor
465 (OMBR) for reuse of wastewater. Water Sci. Technol., 63(8), 1557-1565.
466 9. Elimelech, M. 2006. The global challenge for adequate and safe water. J. Water
467 Supply: Res. Technol. AQUA, 55(1), 3-10.
468 10. Elimelech, M., Chen, W.H., Waypa, J.J. 1994. Measuring the zeta (electrokinetic)
469 potential of reverse osmosis membranes by a streaming potential analyzer.
470 Desalination, 95(3), 269-286.
471 11. Fane, A.G., Wang, R., Hu, M.X. 2015. Synthetic Membranes for Water
472 Purification: Status and Future. Angew. Chem. Int. Ed., 54, 3368-3386.
473 12. Gerrity, D., Pecson, B., Trussell, R.S., Trussell, R.R. 2013. Potable reuse
474 treatment trains throughout the world. J. Water Supply: Res. Technol. AQUA,
475 62(6), 321-338.
476 13. Giwa, A., Hasan, S.W., Yousuf, A., Chakraborty, S., Johnson, D.J., Hilal, N. 2017.
477 Biomimetic membranes: A critical review of recent progress. Desalination, 420,
478 403-424.
479 14. Hai, F.I., Tessmer, K., Nguyen, L.N., Kang, J., Price, W.E., Nghiem, L.D. 2011.
480 Removal of micropollutants by membrane bioreactor under temperature variation.
481 J. Membr. Sci., 383(1), 144-151.
482 15. Holloway, R.W., Regnery, J., Nghiem, L.D., Cath, T.Y. 2014. Removal of trace
483 organic chemicals and performance of a novel hybrid ultrafiltration-osmotic
484 membrane bioreactor. Environ. Sci. Technol., 48(18), 10859-10868.
485 16. Holloway, R.W., Wait, A.S., Da Silva, A.F., Herron, J., Schutter, M.D., Lampi, K.,
486 Cath, T.Y. 2015. Long-term pilot scale investigation of novel hybrid
487 ultrafiltration-osmotic membrane bioreactors. Desalination, 363, 64-74.
488 17. Huang, L., Lee, D.J. 2015. Membrane bioreactor: A mini review on recent R&D

489 works. Bioresour. Technol., 194, 383-388.
490 18. Jensen, M.O., Mouritsen, O.G. 2006. Single-channel water permeabilities of
491 Escherichia coli aquaporins AqpZ and GlpF. Biophys. J., 90(7), 2270-2284.
492 19. Kimura, K., Hara, H., Watanabe, Y. 2005. Removal of pharmaceutical compounds
493 by submerged membrane bioreactors (MBRs). Desalination, 178(1), 135-140.
494 20. Knackmuss, H.J. 1996. Basic knowledge and perspectives of bioelimination of
495 xenobiotic compounds. J. Biotechnol., 513, 287-295.
496 21. Lay, W.C.L., Liu, Y., Fane, A.G. 2010. Impacts of salinity on the performance of
497 high retention membrane bioreactors for water reclamation: A review. Water Res.,
498 44(1), 21-40.
499 22. Li, D., Yan, Y., Wang, H. 2016. Recent advances in polymer and polymer
500 composite membranes for reverse and forward osmosis processes. Prog. Polym.
501 Sci., 61, 104-155.
502 23. Li, X., Chou, S., Wang, R., Shi, L., Fang, W., Chaitra, G., Tang, C.Y., Torres, J.,
503 Hu, X., Fane, A.G. 2015. Nature gives the best solution for desalination:
504 Aquaporin-based hollow fiber composite membrane with superior performance. J.
505 Membr. Sci., 494, 68-77.
506 24. Li, X., Loh, C.H., Wang, R., Widjajanti, W., Torres, J. 2017. Fabrication of a
507 robust high-performance FO membrane by optimizing substrate structure and
508 incorporating aquaporin into selective layer. J. Membr. Sci., 525, 257-268.
509 25. Luo, W., Hai, F.I., Price, W.E., Elimelech, M., Nghiem, L.D. 2016a. Evaluating
510 ionic organic draw solutes in osmotic membrane bioreactors for water reuse. J.
511 Membr. Sci., 514, 636-645.
512 26. Luo, W., Hai, F.I., Price, W.E., Nghiem, L.D. 2015. Water extraction from mixed
513 liquor of an aerobic bioreactor by forward osmosis: Membrane fouling and
514 biomass characteristics assessment. Sep. Purif. Technol., 145(0), 56-62.
515 27. Luo, W., Phan, H.V., Hai, F.I., Price, W.E., Guo, W., Ngo, H.H., Yamamoto, K.,
516 Nghiem, L.D. 2016b. Effects of salinity build-up on the performance and

517 bacterial community structure of a membrane bioreactor. Bioresour. Technol., 200,
518 305-310.
519 28. Luo, W., Phan, H.V., Xie, M., Hai, F.I., Price, W.E., Elimelech, M., Nghiem, L.D.
520 2017. Osmotic versus conventional membrane bioreactors integrated with reverse
521 osmosis for water reuse: Biological stability, membrane fouling, and contaminant
522 removal. Water Res., 109, 122-134.
523 29. Madsen, H.T., Bajraktari, N., Hélix-Nielsen, C., Van der Bruggen, B., Søgaard,
524 E.G. 2015. Use of biomimetic forward osmosis membrane for trace organics
525 removal. J. Membr. Sci., 476, 469-474.
526 30. McCutcheon, J.R., Elimelech, M. 2006. Influence of concentrative and dilutive
527 internal concentration polarization on flux behavior in forward osmosis. J. Membr.
528 Sci., 284(1-2), 237-247.
529 31. Mi, B., Elimelech, M. 2010. Organic fouling of forward osmosis membranes:
530 Fouling reversibility and cleaning without chemical reagents. J. Membr. Sci.,
531 348(1), 337-345.
532 32. Nguyen, N.C., Nguyen, H.T., Chen, S.S., Ngo, H.H., Guo, W., Chan, W.H., Ray,
533 S.S., Li, C.W., Hsu, H.T. 2016. A novel osmosis membrane bioreactor-membrane
534 distillation hybrid system for wastewater treatment and reuse. Bioresour. Technol.,
535 209, 8-15.
536 33. Panswad, T., Anan, C. 1999. Impact of high chloride wastewater on an anaerobic
537 anoxic aerobic process with and without inoculation of chloride acclimated seeds.
538 Water Res., 33(5), 1165-1172.
539 34. Qi, S., Wang, R., Chaitra, G.K.M., Torres, J., Hu, X., Fane, A.G. 2016.
540 Aquaporin-based biomimetic reverse osmosis membranes: Stability and long
541 term performance. J. Membr. Sci., 508, 94-103.
542 35. Seviour, R.J., Mino, T., Onuki, M. 2003. The microbiology of biological
543 phosphorus removal in activated sludge systems. FEMS Microbiol. Rev., 27(1),
544 99-127.

36. Shannon, M.A., Bohn, P.W., Elimelech, M. 2008. Science and technology for water purification in the coming decades. Nature, 452, 301-310.
37. Sutzkover, I., Hasson, D., Semiat, R. 2000. Simple technique for measuring the concentration polarization level in a reverse osmosis system. Desalination, 131(1), 117-127.
38. Tadkaew, N., Hai, F.I., McDonald, J.A., Khan, S.J., Nghiem, L.D. 2011. Removal of trace organics by MBR treatment: The role of molecular properties. Water Res., 45(8), 2439-2451.
39. Tang, C., Wang, Z., Petrinić, I., Fane, A.G., Hélix-Nielsen, C. 2015. Biomimetic aquaporin membranes coming of age. Desalination, 368, 89-105.
40. Uygur, A., Karg, F. 2004. Salt inhibition on biological nutrient removal from saline wastewater in a sequencing batch reactor. Enzyme Microb. Technol., 34, 313-318.
41. van Loosdrecht, M.C.M., Brdjanovic, D. 2014. Anticipating the next century of wastewater treatment. Science, 344(6191), 1452-1453.
42. Wang, X., Chen, Y., Yuan, B., Li, X.F., Ren, Y.P. 2014a. Impacts of sludge retention time on sludge characteristics and membrane fouling in a submerged osmotic membrane bioreactor. Bioresour. Technol., 161, 340-347.
43. Wang, X., Yuan, B., Chen, Y., Li, X.F., Ren, Y.P. 2014b. Integration of micro-filtration into osmotic membrane bioreactors to prevent salinity build-up. Bioresour. Technol., 167, 116-123.
44. Wang, X., Zhao, Y., Yuan, B., Wang, Z., Li, X., Ren, Y. 2016. Comparison of biofouling mechanisms between cellulose triacetate (CTA) and thin-film composite (TFC) polyamide forward osmosis membranes in osmotic membrane bioreactors. Bioresour. Technol., 202, 50-58.
45. Werber, J.R., Osuji, C.O., Elimelech, M. 2016. Materials for next-generation desalination and water purification membranes. Nat. Mater. , 1(5), 16018-16033.
46. Woolard, C.R., Irvine, R.L. 1995. Treatment of hypersaline wastewater in the

573 sequencing batch reactor. Water Res., 29(4), 1159-1168.
574 47. Xiao, D., Tang, C.Y., Zhang, J., Lay, W.C.L., Wang, R., Fane, A.G. 2011.
575 Modeling salt accumulation in osmotic membrane bioreactors: Implications for
576 FO membrane selection and system operation. J. Membr. Sci., 366(1-2), 314-324.
577 48. Xie, W., He, F., Wang, B., Chung, T.-S., Jeyaseelan, K., Armugam, A., Tong, Y.W.
578 2013. An aquaporin-based vesicle-embedded polymeric membrane for low
579 energy water filtration. J. Mater. Chem. A, 1(26), 7592-7600.
580 49. Zhang, B., Song, X., Nghiem, L.D., Li, G., Luo, W. 2017. Osmotic membrane
581 bioreactors for wastewater reuse: Performance comparison between cellulose
582 triacetate and polyamide thin film composite membranes. J. Membr. Sci., 539,
583 383-391.
584 50. Zhao, Y., Qiu, C., Li, X., Vararattanavech, A., Shen, W., Torres, J., Hélix-Nielsen,
585 C., Wang, R., Hu, X., Fane, A.G., Tang, C.Y. 2012. Synthesis of robust and
586 high-performance aquaporin-based biomimetic membranes by interfacial
587 polymerization-membrane preparation and RO performance characterization. J.
588 Membr. Sci., 423-424, 422-428.

589

LIST OF TABLES

Table 1: Key properties of the aquaporin and two conventional FO membranes (average ± standard deviation of triplicate measurements)

Parameters	Aquaporin	CTA	TFC
Pure water permeability (L/m^2h-bar)	2.09 ± 0.02	0.84 ± 0.03	2.50 ± 0.25
Salt (NaCl) permeability (L/m^2h)	0.07 ± 0.01	0.32 ± 0.06	0.19 ± 0.03
Membrane structural parameter (μm)	301 ± 36	575 ± 28	245 ± 35
Observed NaCl rejection (%)	99.9 ± 0.1	92.0 ± 1.4	98.0 ± 0.2
Contact angle (°)	74.5 ± 8.9	60.4 ± 5.2	42.3 ± 3.2
Zeta potential at pH 8 (mV)	-16.4 ± 2.3	-4.5 ± 0.4	-14.2 ± 0.5

LIST OF FIGURES

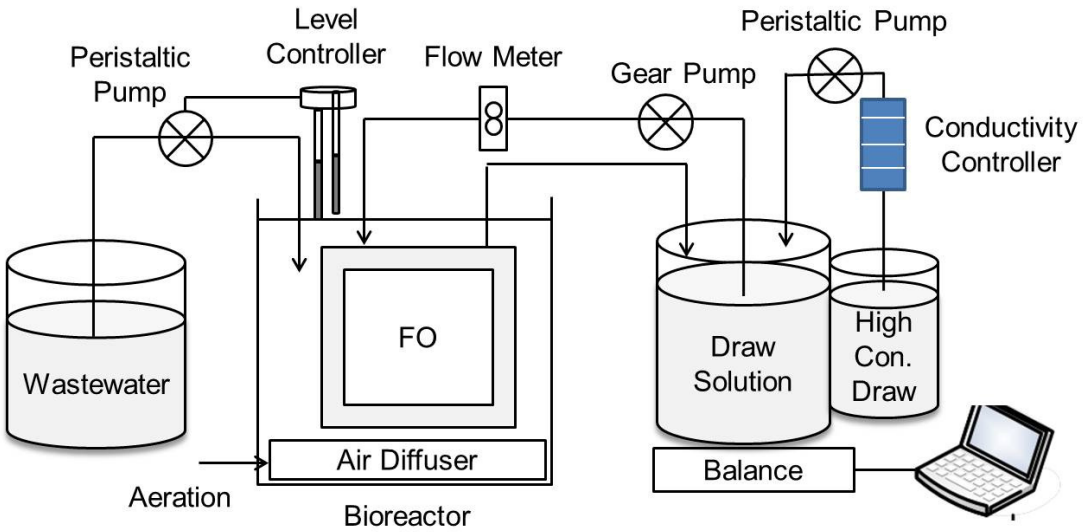

Fig. 1: Schematic diagram of the osmotic membrane bioreactor system.

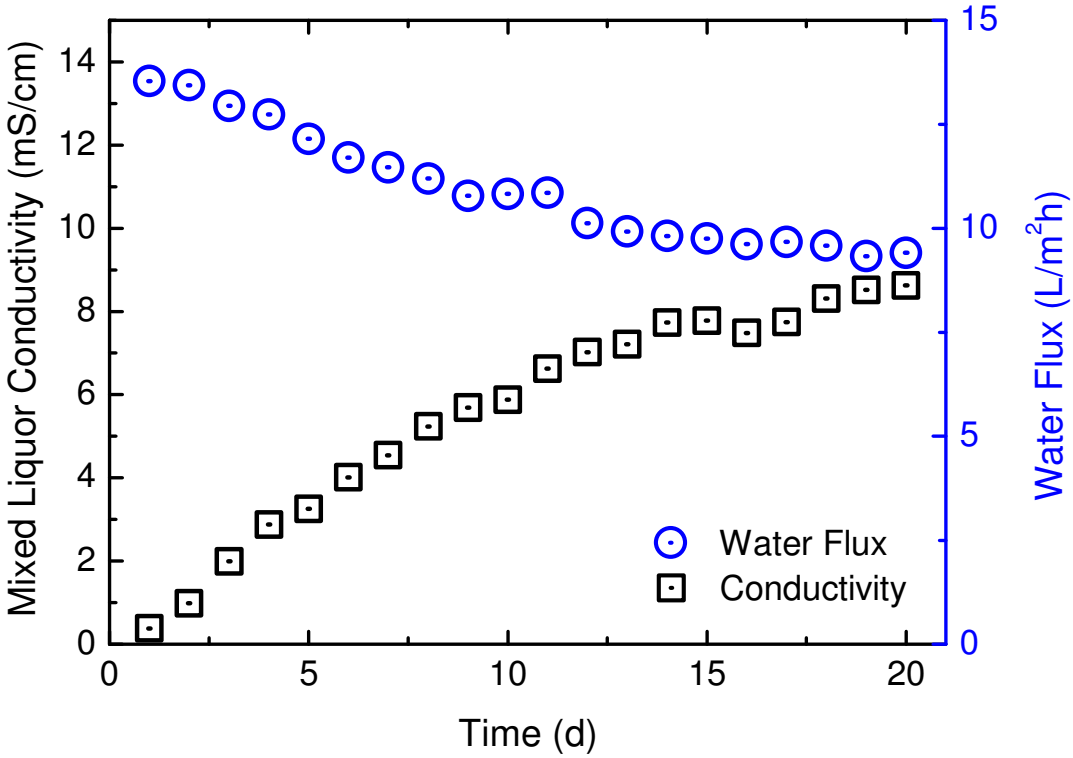

Fig. 2: Mixed liquor conductivity and water flux during OMBR operation using the aquaporin FO membrane. Experimental conditions: draw solution = 0.5 M NaCl; cross-flow velocity = 5.2 cm/s; DO = 2 mg/L; initial MLSS = 6.8 g/L; SRT = 20 d; HRT = 24 – 36 h; temperature = 22 ± 1 ºC.

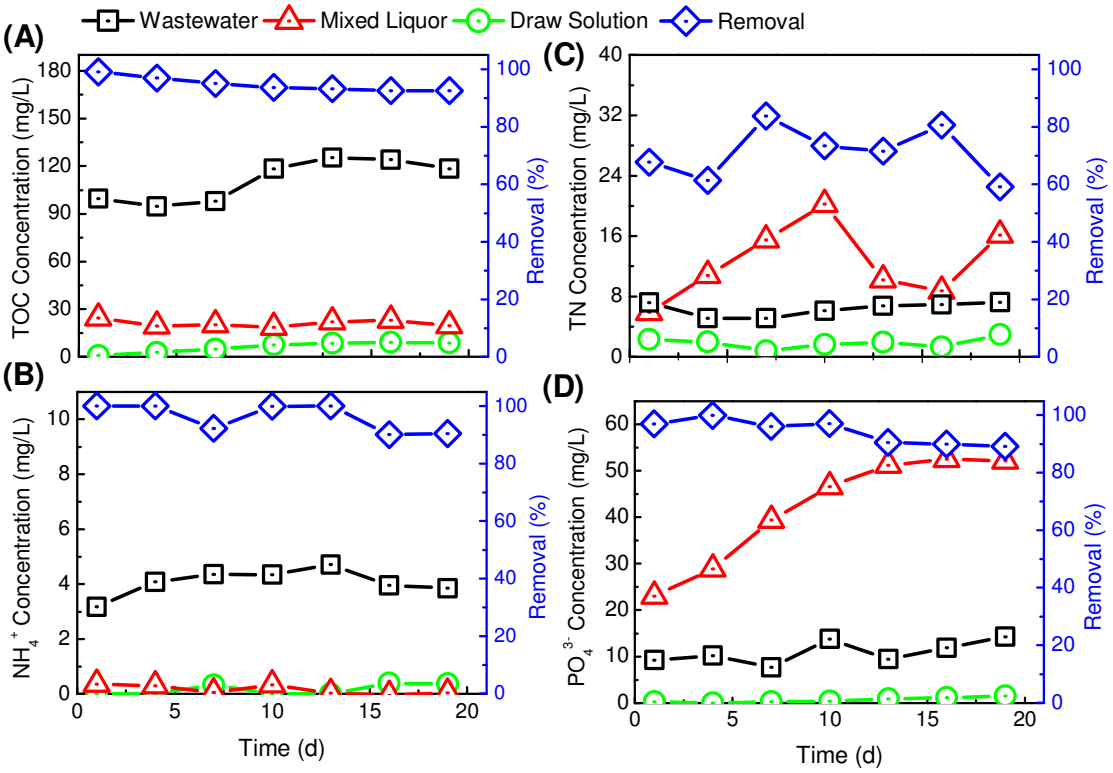

Fig. 3: (A) TOC, (B) TN, (C) NH_4^+, and (D) PO_4^{3-} concentrations as well as their overall removal in OMBR using the aquaporin FO membrane. Experimental conditions are as described in Fig. 2.

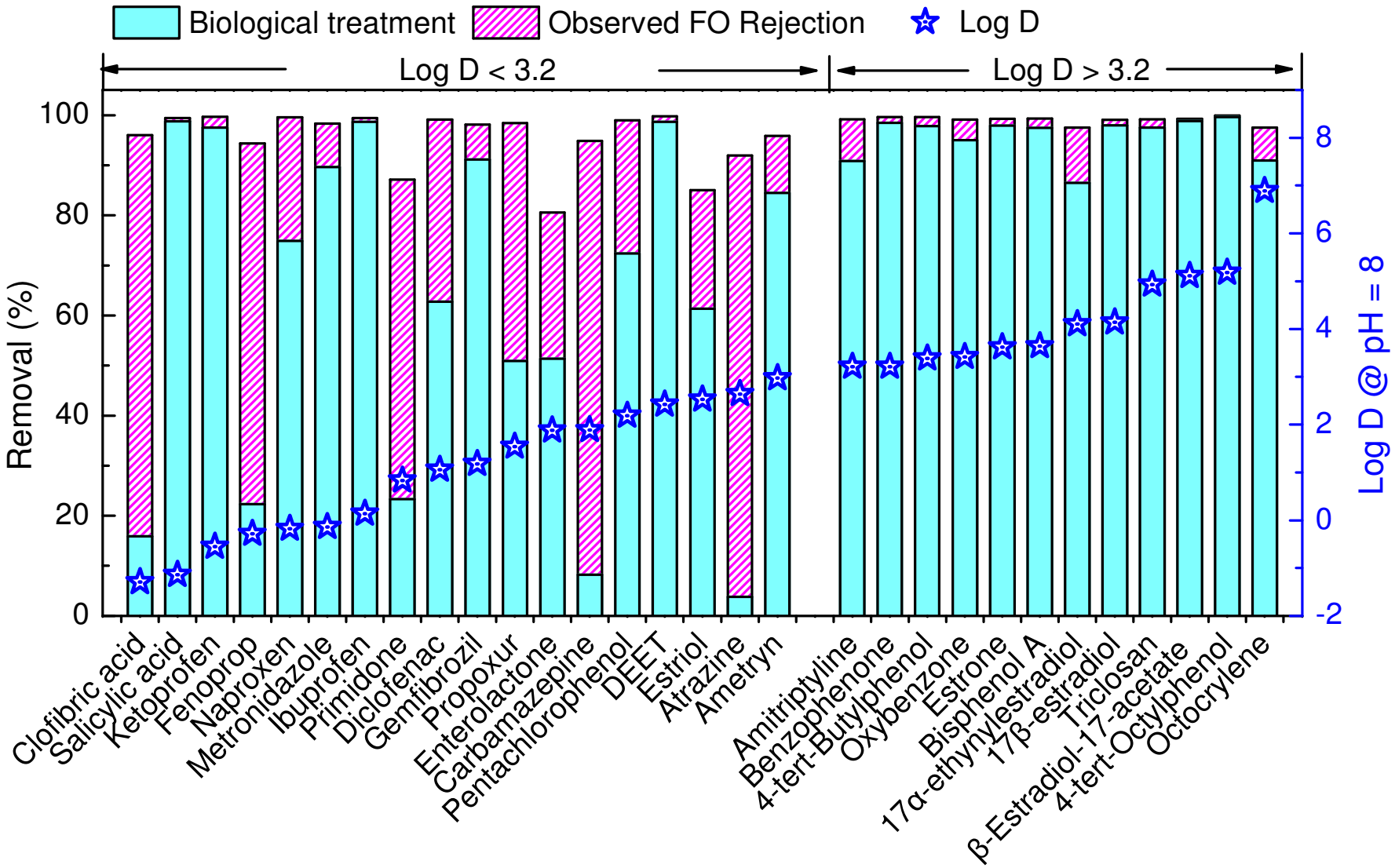
Biological treatment
Observed FO Rejection
Log D
Log D < 3.2
Log D > 3.2
Removal (%)
Log D @ pH = 8
Clofibric acid
Salicylic acid
Ketoprofen
Fenoprop
Naproxen
Metronidazole
Ibuprofen
Primidone
Diclofenac
Gemfibrozil
Propoxur
Enterolactone
Carbamazepine
Pentachlorophenol
DEET
Estriol
Atrazine
Ametryn
Amitriptyline
Benzophenone
4-tert-Butylphenol
Oxybenzone
Estrone
Bisphenol A
17α-ethynylestradiol
17β-estradiol
Triclosan
β-Estradiol-17-acetate
4-tert-Octylphenol
Octocrylene

Fig. 4: Removal of TrOCs by the biological treatment and the FO rejection during OMBR operation using the aquaporin membrane. Average removal data obtained from four measurements (once every 5 days) are shown, with the standard deviation in the range of 0.1 to 30%. TrOCs are ordered according to their effective octanol – water partition coefficient (i.e. Log *D*) at solution pH of 8. The observed FO rejection shows the removal difference between the bioreactor and OMBR. Experimental conditions are as described in Fig. 2.

Supplementary Data

Appendix A

A cross-flow forward osmosis (FO) system was used to determine the water flux and reverse salt flux of different FO membranes. The FO system comprised a cross-flow membrane cell and a draw solution delivery and control unit. The membrane cell was made of acrylic plastic and had two identical flow chambers with length, width, and height of 130, 95, and 2 mm, respectively. The effective membrane area was 123.5 cm^2. Two gear pumps (Micropump, Vancouver, WA) were used to simultaneously circulate the feed and draw solutions to the membrane cell at a cross-flow rate of 1 L/min, corresponding to a cross-flow velocity of 8.8 cm/s. Deionized water and 0.5 NaCl solution was used as the feed and draw solution, respectively. During FO operation, the draw solution concentration was kept constant using the conductivity control equipment and highly concentrated draw solution (6 M NaCl). The draw solution reservoir was placed on a digital balance connected to a computer to determine the water flux of each FO membrane. The system was stabilized for two hours before determining the water flux. The reverse salt flux was determined based on the increase of the feed conductivity and a NaCl calibration curve.

Table S1: Physicochemical properties of the 30 TrOCs investigated in this study.

Compounds	Chemical Formula	Log D at pH 8	MW (g/mol)	Chemical Structure
Clofibric acid	$C_{10}H_{11}ClO_3$	-1.29	214.6	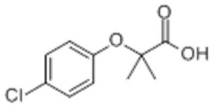
Salicylic acid	$C_7H_6O_3$	-1.14	138.1	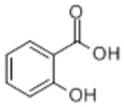

Ketoprofen	$C_{16}H_{14}O_3$	-0.55	254.3	
Fenoprop	$C_9H_7Cl_3O_3$	-0.28	269.5	
Naproxen	$C_{14}H_{14}O_3$	-0.18	230.3	
Metronidazole	$C_6H_9N_3O_3$	-0.14	171.2	
Ibuprofen	$C_{13}H_{18}O_2$	0.14	206.3	
Primidone	$C_{12}H_{14}N_2O_2$	0.83	218.3	
Diclofenac	$C_{14}H_{11}Cl_2NO_2$	1.06	296.2	
Gemfibrozil	$C_{15}H_{22}O_3$	1.18	250.3	
Propoxur	$C_{11}H_{15}NO_3$	1.54	209.2	
Enterolactone	$C_{18}H_{18}O_4$	1.88	298.33	
Carbamazepine	$C_{15}H_{12}N_2O$	1.89	236.3	
Pentachlorophenol	C_6HCl_5O	2.19	266.4	
DEET	$C_{12}H_{17}NO$	2.42	191.3	
Estriol	$C_{18}H_{24}O_3$	2.53	288.4	

Atrazine	$C_8H_{14}ClN_5$	2.64	215.7	
Ametryn	$C_9H_{17}N_5S$	2.97	227.3	
Amitriptyline	$C_{20}H_{23}N$	3.21	277.4	
Benzophenone	$C_{13}H_{10}O$	3.21	182.2	
4-tert-Butylphenol	$C_{10}H_{14}O$	3.39	150.2	
Oxybenzone	$C_{13}H_{10}O$	3.42	228.2	
Estrone	$C_{18}H_{22}O_2$	3.62	270.4	
Bisphenol A	$C_{15}H_{16}O_2$	3.64	228.3	
17α-ethynylestradiol	$C_{20}H_{24}O_2$	4.11	296.4	
17β-estradiol	$C_{18}H_{24}O_2$	4.14	272.4	
Triclosan	$C_{12}H_7Cl_3O_2$	4.93	289.5	
β-Estradiol-17-acetate	$C_{20}H_{26}O_3$	5.11	314.4	
4-tert-Octylphenol	$C_{14}H_{22}O$	5.18	206.3	
Octocrylene	$C_{24}H_{27}N$	6.89	361.5	

Source: SciFinder Scholar (ACS) database.

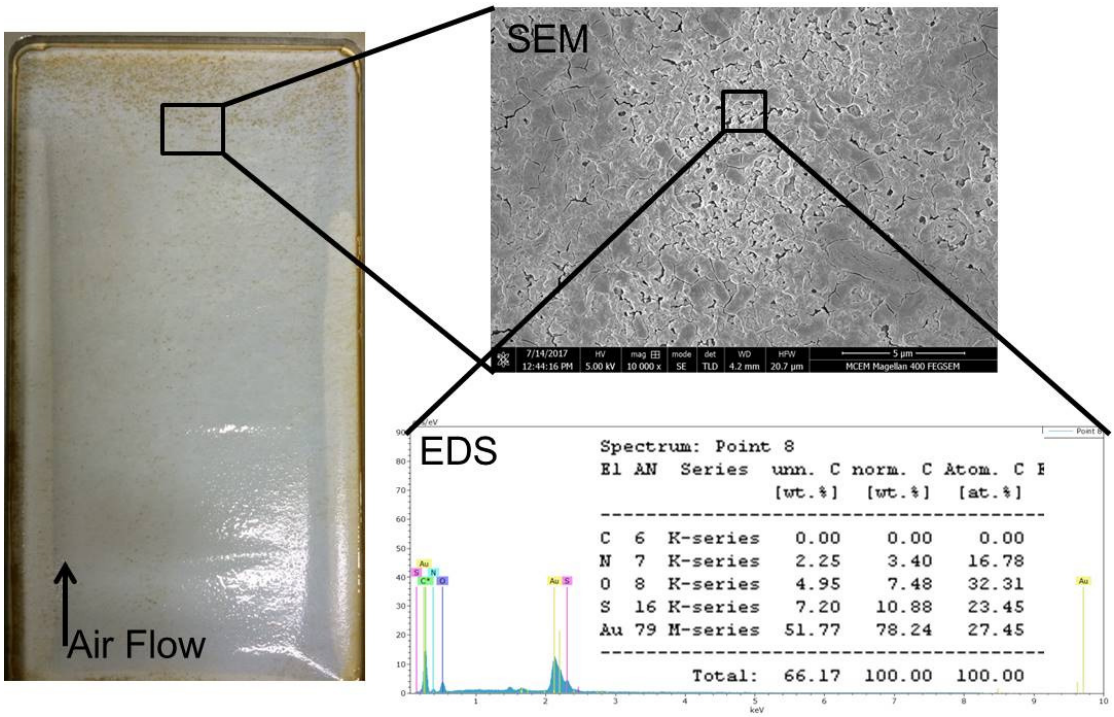

Fig. S1: Photo and SEM-EDS measurement of the aquaporin FO membrane after 20 days of OMBR operation. Experimental conditions: draw solution = 0.5 M NaCl; cross-flow velocity = 5.2 cm/s; DO = 2 mg/L; initial MLSS = 6.8 g/L; SRT = 20 d; HRT = 24 – 36 h; temperature = 22 ± 1 ºC.

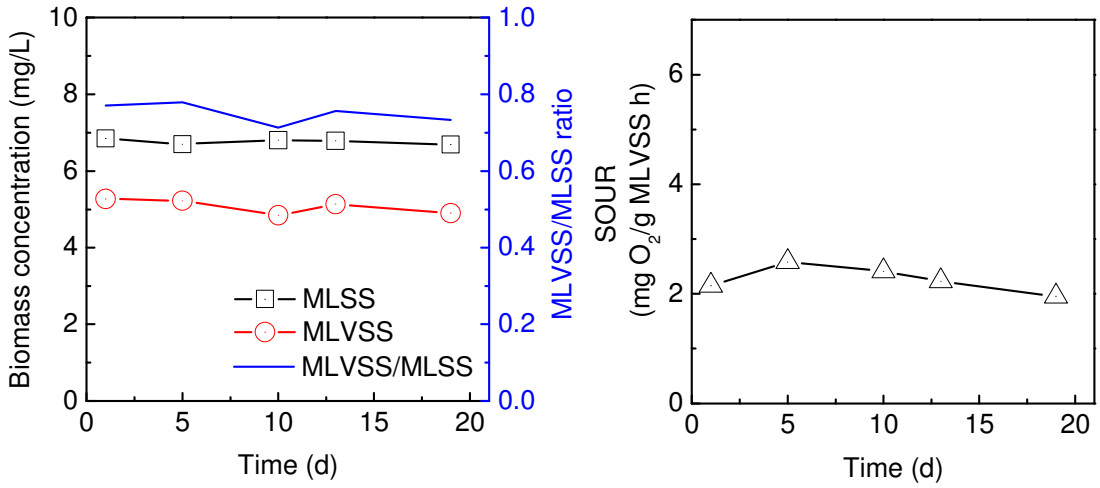

Fig. S2: Biomass concentration and specific oxygen uptake rate (SOUR) of sludge

during OMBR operation using the aquaporin FO membrane. Mixed liquor suspended solids (MLSS) and mixed liquor volatile suspended solids (MLVSS) concentrations were analyzed based on Standard Method 2540 (APHA, 2005). SOUR was determined based on Standard Method 1683 (APHA, 2005) to indicate biomass activity. Experimental conditions are shown in Fig. S1.

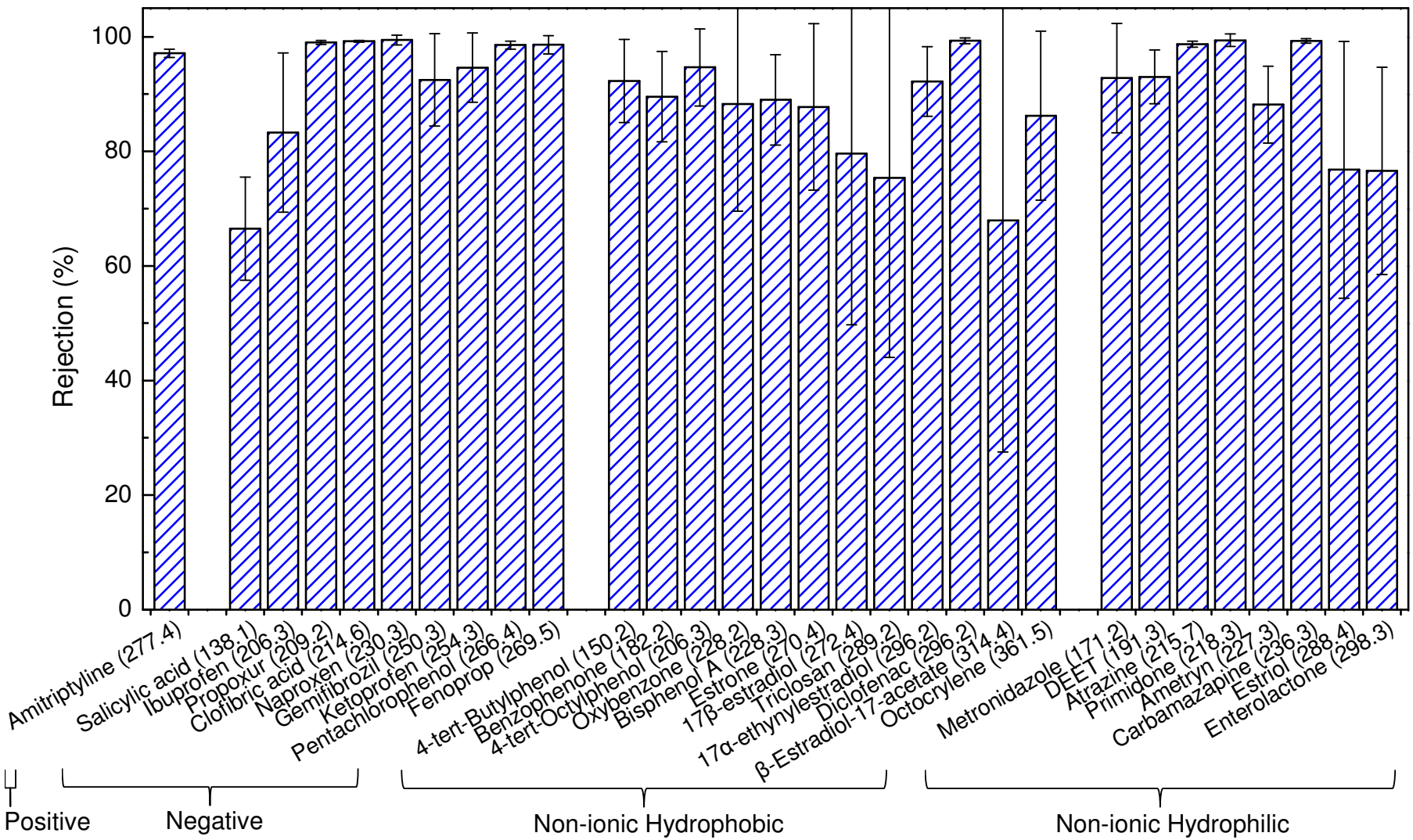
Rejection (%)
0
20
40
60
80
100
Amitriptyline (277.4)
Salicylic acid (138.1)
Ibuprofen (206.3)
Propoxur (209.2)
Clofibric acid (214.6)
Naproxen (230.3)
Gemfibrozil (250.3)
Ketoprofen (254.3)
Pentachlorophenol (266.4)
Fenoprop (269.5)
4-tert-Butylphenol (150.2)
Benzophenone (182.2)
4-tert-Octylphenol (206.3)
Oxybenzone (228.2)
Bisphenol A (228.3)
Estrone (270.4)
17β-estradiol (272.4)
Triclosan (289.2)
17α-ethynylestradiol (296.2)
Diclofenac (296.2)
β-Estradiol-17-acetate (314.4)
Octocrylene (361.5)
Metronidazole (171.2)
DEET (191.3)
Atrazine (215.7)
Primidone (218.3)
Ametryn (227.3)
Carbamazapine (236.3)
Estriol (288.4)
Enterolactone (298.3)
Positive
Negative
Non-ionic Hydrophobic
Non-ionic Hydrophilic

Fig. S3: Rejection of TrOCs by the aquaporin FO membrane over OMBR operation. Error bars represent the standard deviation from four measurements (once every 5 days). Molecular weight (g/mol) of each compound is shown in the parenthesis. Based on their Log *D* values at solution pH 8, non-ionic compounds were grouped as hydrophilic (Log $D < 3.2$) and hydrophobic (Log $D > 3.2$). Experimental conditions are as described in Fig. S1.

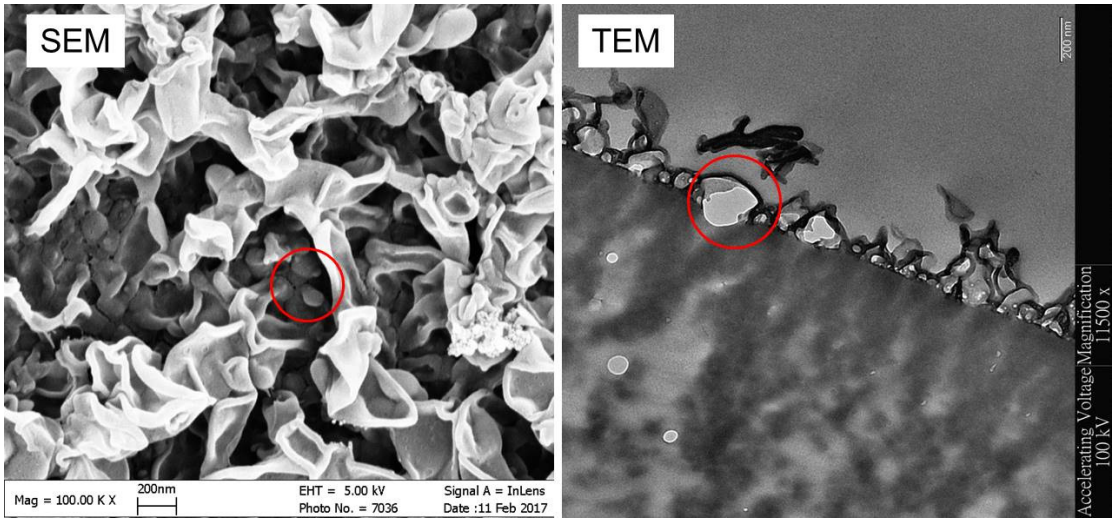

Fig. S4: Scanning electron microscopy (SEM) of the surface and transmission electron microscopy (TEM) of the cross-section of the pristine aquaporin FO membrane. Round-shape nodules, possibly proteoliposomes with aquaporin proteins, were representatively marked in red cycles. Prior to the SEM measurement, air-dried membrane samples were coated with an ultra-thin layer of gold using a sputter coater (SPI Module, West Chester, PA). Membrane samples for TEM were dehydrated by several changes of ethanol (3 times 100% ethanol, 15 min for each step). Samples were then infiltrated in 50, 67, and 100% LR White resin (volumetric %, prepared in ethanol) sequentially, followed by embedding them in fresh LR White resin that was subsequently polymerized at 48 °C for 3 days. After complete polymerization of the resin, thin TEM sections (<100 nm thickness) were cut with a diamond knife using Leica Ultracut S ultramircotome (Leica, Wetzlar, Germany) and transferred onto copper TEM grids for imaging at an accelerating voltage of 80 keV.

Reference

APHA. 2005. Standard methods for the examination of water and wastewater. APHA-AWWA-WEF. 9780875530475, 0875530478.